Photochemistry and Photobiology, 2010, 86: 580–585

Use of UV-A Energy for Photosynthesis in the Red Macroalga *Gracilaria lemaneiformis*

Juntian Xu[1,2] and Kunshan Gao*[1]

[1]State Key Laboratory of Marine Environmental Science, Xiamen University, Xiamen, China
[2]Key Lab of Marine Biotechnology of Jiangsu Province, Huaihai Institute of Technology, Lianyungang, China

Received 23 September 2009, accepted 28 December 2009, DOI: 10.1111/j.1751-1097.2010.00709.x

ABSTRACT

UV radiation is known to inhibit photosynthetically active radiation (PAR)-driven photosynthesis; however, moderate levels of UV-A have been shown to enhance photosynthesis and growth rates of some algae. Here, we have shown that UV-A alone could drive photosynthetic utilization of bicarbonate in the red alga *Gracilaria lemaneiformis* as evidenced in either O_2 evolution or carbon fixation as well as pH drift. Addition of UV-B inhibited the apparent photosynthetic efficiency, raised the photosynthetic compensation point and photosynthesis-saturating irradiance level, but did not significantly affect the maximal rate of photosynthetic O_2 evolution. The electron transport inhibitor, DCMU, inhibited the photosynthesis completely, reflecting that energy of UV-A was transferred in the same way as that of PAR. Inorganic carbon acquisition for photosynthesis under UV alone was inhibited by the inhibitors of carbonic anhydrase. The results provided the evidence that *G. lemaneiformis* can use UV-A efficiently to drive photosynthesis based on the utilization of bicarbonate, which could contribute significantly to the enhanced photosynthesis in the presence of UV-A observed under reduced levels of solar radiation.

INTRODUCTION

Solar UV radiation (UVR, 280–400 nm) is a major stress factor for many phototrophic organisms in aquatic and terrestrial ecosystems (1). Increased UV-B irradiance (280–315 nm) caused by the reduction of ozone can induce additional damage to aquatic photosynthetic organisms (2). Although the chlorine concentration in the stratosphere has decreased, following the implementation of the Montreal Protocol, the time required for recovery of the ozone layer is uncertain and will depend on the influences of climate change on the stratosphere (3). Solar UVR is known to play important roles in affecting the biological activities of algae or cyanobacteria in negative and/or positive ways. It can inhibit photosynthesis (4,5), damage photosystem II reaction center subunits (6) and DNA molecule (7), alter morphology (8,9), reduce nutrient uptake rate (10) and change community structure (11). It can also affect the early development (12,13) and spore germination (14,15) of macroalgae. On the other hand, UV-A is shown to play positive roles in photo-repairing UVB-induced damages (7) and enhancing photosynthesis in phytoplankton (5,16,17) and in the macroalga *Gracilaria lemaneiformis* (18). Reduced levels of UV-A radiation have been found to enhance the growth of the brown alga *Fucus gardneri* embryos (13). On the other hand, insignificant (neutral) effects of UVR have also been reported on the growth of *Ulva rigida* (19) and *Fucus serratus* (20) during long-term experiments.

In the red alga *G. lemaneiformis*, we showed previously that the presence of UV-A at moderate levels (about 10 W m^{-2}) increased the net photosynthesis and resulted in higher apparent photosynthetic efficiency under natural solar radiation (18). This species has been found to be able to use bicarbonate as the major inorganic carbon for photosynthesis (21). There is a possibility that UV-A can drive utilization of bicarbonate for photosynthesis in this red macroalga. In phytoplankton, enhanced photosynthetic carbon fixation in the presence of UV-A was also found on cloudy days, suggesting that UV-absorbing compounds play a role in capturing the UV energy (17). However, little evidence has been documented to support this hypothesis. O_2 evolution under UV-alone radiation has been detected in some green and red macroalgae (22–25). On the other hand, UV-B was shown to increase the intracellular dissolved inorganic carbon (DIC) pool in the green microalga *Dunaliella tertiolecta* (26), and the activity of extracellular periplasmic carbonic anhydrase (CA) in the diatom *Skeletonema costatum* (Greville) Cleve was stimulated by both UV-A and UV-B (27), suggesting that UV could affect inorganic carbon acquisition processes by these microalgae. Contrastingly, little is known of this aspect in macroalgae (28). In *G. lemaneiformis*, both stimulation and inhibition of photosynthesis by UV-A were reported under natural solar radiation. Therefore, we designed further experiments to test how UV-A functions to bring about the positive and negative effects under UV-alone or in combination with photosynthetically active radiation (PAR).

MATERIALS AND METHODS

Plant materials. Thalli of *G. lemaneiformis* Bory were collected in March 2007 from the coastal waters of Nanao island, Shantou (116.6°E, 23.3°N), where they were farmed at a depth of 0.5–1 m and exposed to UVA of 0–70 W m^{-2} and to UV-B of 0–2.4 W m^{-2}. Plants were cleaned of epiphytes and maintained in the laboratory for about 1 week with natural seawater (30‰ salinity, enriched with 60 μM $NaNO_3$ and 4 μM NaH_2PO_4) at 20°C, and 60 μmol photons $m^{-2}s^{-1}$ of PAR (12:12 LD).

*Corresponding author email: ksgao@xmu.edu.cn (Kunshan Gao)

Radiation treatments and measurements. The thalli were exposed to different radiation treatments under a solar simulator (Sol 1200 W; Dr. Hönle Martinsried, Germany). To allow the thalli to receive UVR alone, they were placed in quartz tubes and then maintained in an opaque plastic box, in the top of which a PAR cutoff filter, UG11 (Schott, Mainz, Germany), was sealed. The photosynthesis–light (P–E) curves were obtained in the absence of PAR under no and up to five layers of neutral density screens so that UVR irradiance varied from 55% to 5% (UV-A, 25.5, 15.9, 8.8, 4.8 and 2.8 Wm^{-2}; UVR, 32.8, 20.5, 11.3, 6.2 and 3.6 Wm^{-2}). The exposures were either under UV-A + UV-B or UV-A alone. For the UV-A-alone treatments, a Folex 320 cutoff foil (Montagefolie, Nr. 10155099; Folex, Dreieich, Germany) was attached at the top of the UG11 filter to screen off UV-B irradiance. For the UV-A + B treatment, UV-C from the xenon lamp was screened off using the Ultraphan 295 foil (UV Opak; Digefra, Munich, Germany). The transmission spectra of the cutoff filters are shown in Fig. 1. The UG11 filter cuts off 100% PAR and transmits 53.7% of UV-A and 63.8% of UVB. The Folex 320 cutoff foil transmits 70.5% of UV-A, and Ultraphan 295 transmits 85.6% of UV-A and 71.2% of UV-B.

The emission spectra of the solar simulator are published elsewhere (29). Irradiances of UV-B (280–315 nm), UV-A (315–400 nm) and PAR (400–700 nm) were measured with a broadband solar radiometer (ELDONET; Real Time Computer, Inc., Germany). This instrument measures direct and indirect radiation at 1 s intervals (Ulbrich integrating sphere) and records the means over 1-min intervals (30).

pH drift experiments under UVR-only and PAR-alone conditions. *G. lemaneiformis* thalli (about 0.3 g) were placed in a water-jacketed quartz (for UV exposure) or glass (for PAR alone exposure) tubes containing 15 mL filtered natural seawater. The initial pH of the seawater was quickly adjusted to 8.0 with 0.05 M HCl. The thalli with the seawater in the quartz tubes were then exposed to UV or PAR-alone treatments. Three irradiance levels (at the surface of the thalli) were set at 15.9, 25.5 or 31.9 W m^{-2} for UV-A, and at 20.5 (19.2 for UV-A), 32.8 (30.8 for UV-A) or 41.1 (38.6 for UV-A) Wm^{-2} for UV-A + UV-B, respectively. PAR level was set at about 40 W m^{-2} (200 μmol m^{-2} s^{-1}). Changes in pH of the medium were monitored every 2 h for up to 8 h with an ORION 420A pH electrode, which was calibrated with standard NBS buffer. The temperature was controlled at 20 ± 0.5°C using a cooling unit (CAP-3000; Rikakikai, Tokyo, Japan).

Photosynthetic oxygen evolution measurements. Photosynthetic O_2 evolution under UV alone was measured by using a Clark-type oxygen electrode (YSI Model 5300), which was inserted in a water-jacketed quartz vessel of 12 mL for temperature control at 20°C using the cooling unit. The thalli were cut into small segments (about 1.0 cm long) and incubated in filtered natural seawater for at least 1 h to minimize the effect of the cutting damage before transferring to the reaction chamber for measurement. About 0.1 g fresh samples were transferred to the quartz vessel containing 8 mL fresh seawater, which was magnetically stirred. Photosynthetic O_2 evolution under PAR alone was measured in a water-jacketed glass vessel of 12 mL under a halogen lamp which emitted negligible amount of UV unreachable to the thalli due to the glass shield. Parameters for P–E curves were analyzed according to Jassby and Platt (31): $P = P_{max}\tanh(\alpha E/P_{max}) + R_d$, where P represents photosynthetic rate; E, irradiance; P_{max}, the light-saturated photosynthetic rate; α, initial slope at limiting irradiances and R_d, the dark respiration rate.

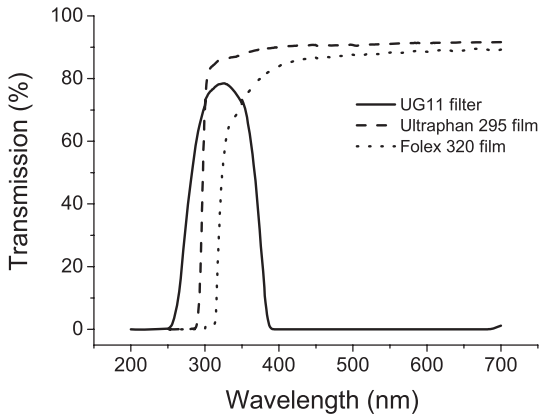

Figure 1. Transmission spectra of the cutoff filters used.

Application of physiological inhibitors. The inhibitors (Sigma), acetazolamide (AZ), 6-ethoxyzolamide (EZ), 4,4′-diisothiocyano-stilbene-2,2′-disulfonate (DIDS) and 3-(3,4-dichlorophenyl)-1, 1-dimethylurea (DCMU) were used to examine Ci-acquisition and O_2 evolution processes. AZ inhibits the activity of extracellular (periplasmic) CA, not penetrating into cells and only acting on surface-accessible CA (32). EZ penetrates into the cell, inhibiting both external and internal CA. DIDS inhibits the direct uptake of HCO_3^- (33). AZ, EZ and DIDS solutions were applied at final concentrations of 200, 200 and 400 μM, respectively. The stock solution of AZ and EZ (50 mM) was prepared in 0.05 M NaOH and that of DIDS (50 mM) by dissolving it in distilled water. DCMU inhibits reduction of the quinone pool through the Q_B-site of photosystem II, and it was used at a concentration of 10^{-5} M.

Photosynthetic carbon-fixation measurements. Photosynthetic carbon-fixation rates were determined on the basis of Ci removal from the seawater. About 0.1 g thalli were placed into each quartz tube containing 15 mL filtered seawater. Incubations of the tubes were carried out for 1 h under UV-A or UV-A + B treatment (UV-A, 25.5 W m^{-2}; UVR, 32.8 W m^{-2}). [DIC] of seawater was measured by a total organic carbon (TOC) meter (TOC-5000; Shimadzu Corp., Kyoto, Japan), which automatically measures both total inorganic carbon (DIC) and total carbon in a liquid. The photosynthetic carbon-fixation rates was estimated from the following equation: $Pn = V \times (C1 - C2)/T/FW$, where V is the volume of seawater, $C1$ and $C2$ are DIC concentrations of seawater before and after the incubation over a period of T (min), respectively; FW is the fresh weight of the thalli.

Experiments on the coeffect of UVR and PAR. To examine the coeffect of UVR and PAR, we set up five radiation treatments: UV-A, UV-A + B, PAR, PAR + UV-A, PAR + UV-A + B, which were carried out on a cloudy (30 March 2007) and a sunny day (30 April 2007), respectively. The measurements were performed during the noon. About 0.1 g thalli were placed into each quartz tube containing 15 mL filtered seawater and the tubes were placed under the radiation treatments for 1 h, and the photosynthetic carbon-fixation rates were determined as mentioned above. The intensity of the UV-A or UV-B bands was achieved equally under different radiation treatments using the UG11 filter and/or the neutral density screens.

Data treatment and statistic analysis. The data were expressed as the means ± standard deviation (SD). Statistical significance of the data was tested with one-way analysis of variance (ANOVA, Tukey test) or paired t-test (P–E curve for UV). A confidence level of 95% was used in all analyses.

RESULTS

The pH in the cultures of *G. lemaneiformis* thalli under either UV-A or UV-A + B increased with time (Fig. 2). Under UVA-alone treatments, the pH showed the highest values at a moderate level of UV-A (Fig. 2A), being significantly ($P < 0.01$) higher than the lowest level of UVA. In the presence of UV-B, the highest pH values were observed at the lowest irradiance level, reflecting a UVB-induced inhibition of photosynthetic carbon fixation (Fig. 2B). Under equivalent energy levels (32–33 W m^{-2}) of UV-A or UVA+B, the end pH in the cultures was about 0.33 higher in the thalli exposed to UV-A alone than those exposed to UV-A + B. The pH under PAR alone also increased with time and reached a compensation point at pH 9.4 after 8 h (Fig. 2C).

When photosynthetic O_2 evolution of *G. lemaneiformis* was measured under UV-A alone or UV-A + B irradiation at different intensities (Fig. 3), the net photosynthetic rate was positive above the irradiance level of about 8 W m^{-2}. The net photosynthetic rate increases with increased irradiance of either UV-A or UV-A + B, reflecting an energy-dependent

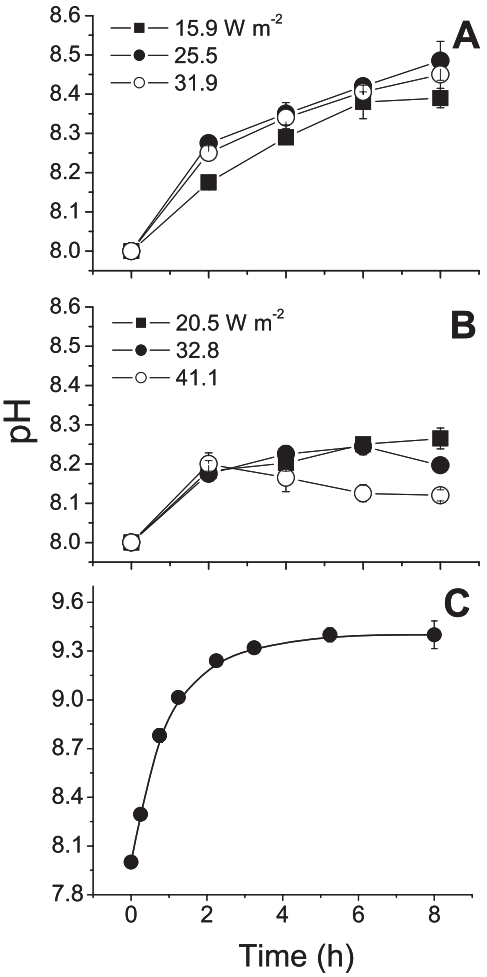

Figure 2. The pH drift in the cultures of *Gracilaria lemaneiformis* thalli under UV-A alone (A), under UV-A + B (B) or under PAR alone (C). Vertical bars represent ±standard deviation of the means ($n = 3$).

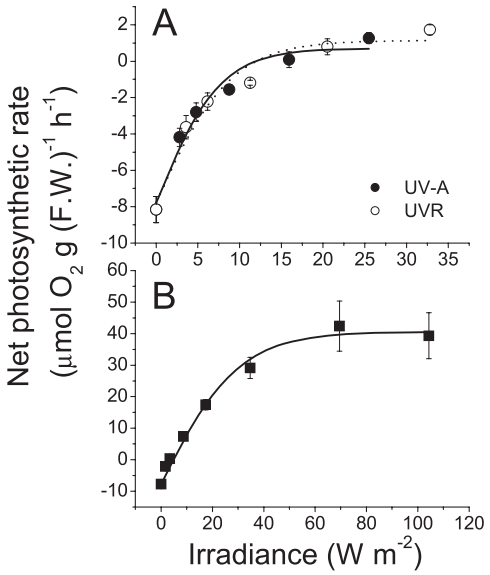

Figure 3. Photosynthetic O_2 evolution of *Gracilaria lemaneiformis* as a function of UV-A or UV-A + B (A) and PAR (B). Vertical bars represent ±standard deviation of the means ($n = 5$).

Table 1. Photosynthetic parameters of the P–E curves in *Gracilaria lemaneiformis* under UV-A, UV-A + UV-B or PAR irradiances, derived from Fig. 3.

	UV-A	UVR	PAR
P_m (μmol O_2 g^{-1} FW h^{-1})	8.51 ± 0.72 a	8.91 ± 0.70 a	48.41 ± 7.75 b
R_d (μmol O_2 g^{-1} FW h^{-1})	−7.74 ± 0.75 a	−7.74 ± 0.75 a	−7.73 ± 0.38 a
α ([μmol O_2 g^{-1} FW h^{-1}]/W m^{-2})	1.12 ± 0.12 a	0.99 ± 0.09 b	1.61 ± 0.06 c
E_C (W m^{-2})	6.97 ± 0.57 a	7.77 ± 0.58 b	4.74 ± 0.21 c
E_K (W m^{-2})	7.63 ± 0.94 a	8.97 ± 0.84 b	29.72 ± 4.82 c

P_m = maximum net photosynthetic rate; R_d = dark respiration rate; a = photosynthetic efficiency; E_C = light compensation point; E_K = light saturation point. Different letters show significant ($P < 0.05$) differences among the treatments for each parameter. Data are means ± SD ($n = 5$).

UV-A-driven photosynthesis. The photosynthesis–UV-A relationship fits into the classic P–E relation, $P = Pm*\tanh(\alpha E/Pm) + R_d$. No significant ($P > 0.1$) difference was found in the P_{max} between UV-A and UV-A + B treatments over a period of 30 min measurements (Table 1). Dark respiration (−7.74 ± 0.75 μmol O_2 g^{-1} FW h^{-1}) of the thalli prior to the radiation treatments was identical, reflecting their equal physiological status at the beginning of the measurements. The apparent photosynthetic efficiency α was significantly higher ($P < 0.01$), while the photosynthetic compensation point (E_C) and saturating point (E_K) were lower ($P < 0.05$), compared with that under the UV-A + B treatment. In contrast, the thalli under PAR alone exhibited about 5.7 times higher photosynthetic rates than under UV-A alone. The α and E_K values were lower while E_C was higher in the thalli exposed to UV-A alone or UVA + B than under PAR alone.

When DCMU, an inhibitor of photosynthetic electron transport, was added, the UV-A-driven photosynthetic O_2 evolution (Fig. 4A) or carbon fixation was not observed (Fig. 4B). Addition of the CA inhibitors AZ (inhibiting extracellular CA) and EZ (inhibiting both intracellular and extracellular CA) caused a significant ($P < 0.01$) decline in O_2 evolution of the thalli irradiated with UV-A or UV-A + B (Fig. 5A) similar to the effects in the thalli irradiated with PAR only (Fig. 5B). Addition of DIDS, the anion exchange inhibitor, led to zero photosynthetic O_2 evolution under UV, but did not affect the photosynthesis under PAR alone (Fig. 5B). The photosynthetic rates of *G. lemaneiformis* did not change in the presence of the anion exchanger inhibitor DIDS (Fig. 5B). The absorption of UV energy by DIDS made it impossible to see if there is any UV-pumped HCO_3^- uptake for photosynthesis (Fig. 5C).

On the cloudy day (Fig. 6A), photosynthetic carbon fixation rate was not significantly different under UV-A and UV-A + B ($P > 0.05$), achieving 17% of the PAR-driven rate (Fig. 6B). On the sunny day (Fig. 6C), photosynthetic carbon fixation rate of the thalli under UV-A was significantly higher ($P < 0.05$) than that under the UV-A + B condition (Fig. 6B). The presence of UV-A or UVA + B significantly ($P < 0.05$) enhanced the net photosynthetic carbon fixation rate compared with the PAR alone treatment on the cloudy

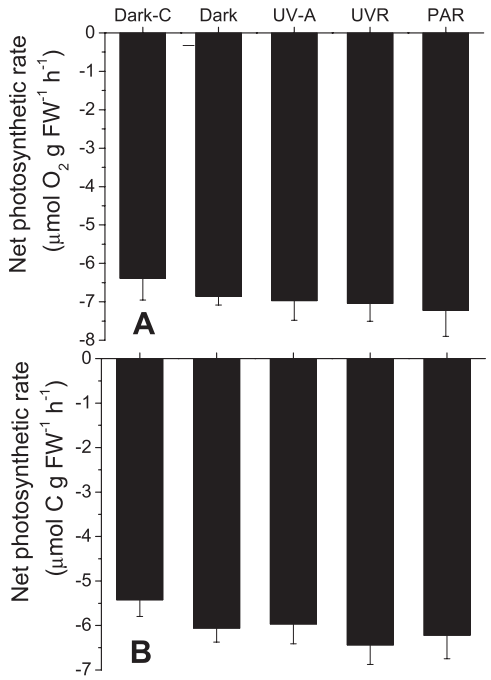

Figure 4. Rate of net photosynthetic O_2 evolution (A) and net photosynthetic carbon fixation rate (B) of *Gracilaria lemaneiformis* thalli incubated in the presence of 10^{-5} M DCMU under dark and irradiation of UV-A (25.5 W m^{-2}), UV-A + B (32.8 W m^{-2}) or PAR (360 W m^{-2}), respectively. "Dark-C" represents the thalli under darkness in the absence of DCMU. Vertical bars represent ±standard deviation of the means (n = 3).

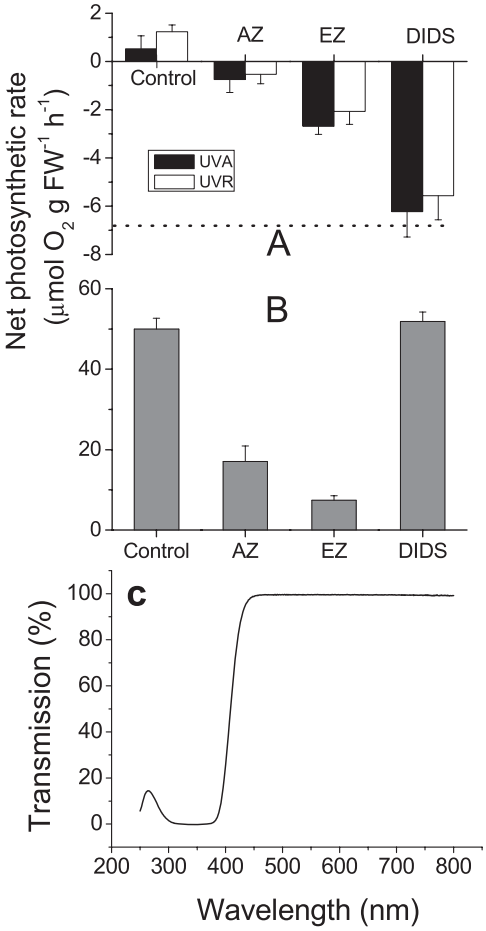

Figure 5. Effects of CA inhibitors (AZ and EZ, 200 μM) and anion exchanger inhibitor (DIDS, 400 μM) on the photosynthetic O_2 evolution rate of *Gracilaria lemaneiformis* under UV-A or UV-A + B radiation (A) and PAR condition (B). Note addition of 400 μM DIDS absorbed almost all of the UV irradiances (C). Vertical bars represent ±standard deviation of the means (n = 6). The dot line represents dark respiration of *G. lemaneiformis*, with the value of 6.8 ± 0.7 μmol O_2 g(F.W.)$^{-1}$ h^{-1}.

day, but both UV-A and UV-B brought about significant reductions ($P < 0.05$) in the rate on the sunny day (Fig. 6D).

DISCUSSION

Evidence of UV-driven photosynthesis in *G. lemaneiformis*

UV-A drove O_2 evolution and carbon fixation in the red alga *G. lemaneiformis*. This indicates that the alga can use the energy of UV-A for photosynthesis. This result is consistent with the evidence from the action spectra of photosynthesis in *Chaetoceros gracilis*, *Glenodinium* sp., *Porphyridium cruentum*, *Chroomonas* sp. and *Ulva* sp. that longer waveband (375 nm–400 nm) of UV-A triggered photosynthetic O_2 evolution (22,23). Halldal (24) reported that photosynthesis was detected in the UV band down to 313 nm in the green alga *Ulva lactuca* and to 300 nm in the red alga *Trailliella intricate*. In the present work, inhibition of the reduction in the quinone pool through the Q_B site of photosystem II with DCMU led to complete inhibition of photosynthetic O_2 evolution and carbonic fixation under UV-A, indicating that the energy was transferred through the electron transport chain of PSII in the same way as PAR. Additionally, UV-A led to enhanced apparent photosynthetic efficiency (α), reflecting that UV-A contributed to the increase in the photosynthetic rate when the energy of PAR was limiting. The presence of UV-B decreased the apparent photosynthetic efficiency of UV-A, reflecting that UV-B harmed the photosystems that use the transferred UV-A energy. Therefore, photosynthetic UV-A compensation and saturating points increased in the presence of UV-B. In contrast, PAR-driven photosynthesis showed higher rate and lower light compensation point. The less efficient use of UV-A than PAR can be attributed to less capturing efficiency of UV-A and its simultaneous harm to the photosynthetic machinery.

Photosynthetic utilization of HCO_3^- by seaweeds is achieved by either dehydration of HCO_3^- to CO_2 catalyzed by extracellular (periplasmic) CA or by direct HCO_3^- uptake, which is then converted to CO_2 with the catalysis of intracellular CA (34,35). Such a utilization of HCO_3^- also works well for the UV-driven photosynthesis as evidenced in the pH drift (Fig. 2) and using the CA inhibitors (Fig. 5A).

The UV-A energy could be captured in several ways. In the haptophyte *Phaeocystis antarctica*, the observed fluorescence emitted from Chl *a* caused by absorption of UV was related to photosynthetic pigments (36). In addition, the energy of UV-A could be directly absorbed by Chl *a*, which also has absorption tails near the UV band (37). Absorbed UV energy was found to generate chlorophyll fluorescence in the diatom *Pseudo-nitzschia multiseries* (38). The energy of UV-A could also be

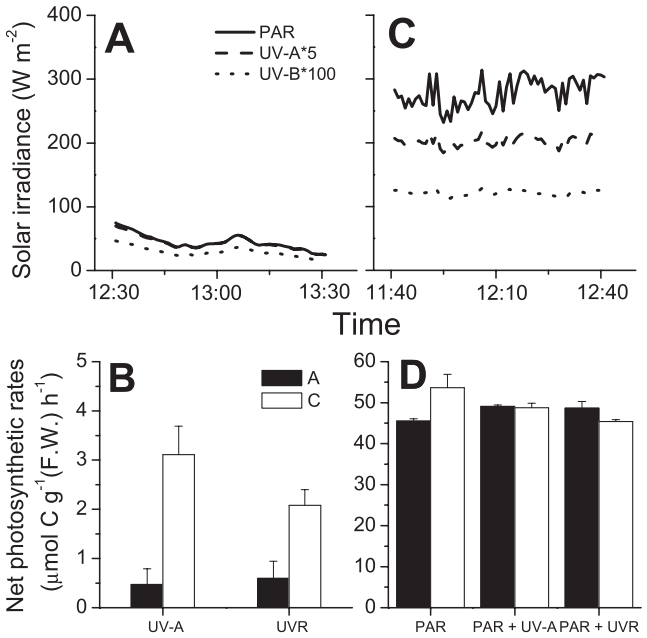

Figure 6. Net photosynthetic carbon fixation rate of *Gracilaria lemaneiformis* under UV-only condition (B) and PAR, PA and PAB treatments (D) in the noon of cloudy day (A) and sunny day (C). (A) On 30 March 2007, the thalli received noontime PAR, UV-A and UV-B by 44, 8.6 and 0.3 W m^{-2}, respectively. (C) On 1 April 2007, the thalli received noontime PAR, UV-A and UV-B by 278, 41 and 1.2 W m^{-2}, respectively. The dark respiration of all treatments was about 8 μmol C g(F.W.)$^{-1}$ h^{-1}. Vertical bars represent $\pm$standard deviation of the means (n = 5).

absorbed by phycobiliproteins. Phycobiliproteins, having small absorption peaks within the UV band, are the main accessory photosynthetic pigments in red algae. Neori *et al.* (22,23) suggested that phycobiliproteins were responsible for the absorption of UV and subsequent photosynthetic O_2 evolution in the tested micro- and macro- red algae. The peaked photosynthetic O_2 evolution within the UV band observed in the red alga *Trailliella intricata* coincided with the UV-absorption peak around 360–390 nm by phycoerythrin (24). Mycosporine-like amino acids (MAAs) are known to absorb UV-A with the absorption range of 310–360 nm. Red algae often exhibit high levels of MAAs (39), which have been suggested to function as the antenna pigments channeling the energy to the photosynthetic apparatus (17,40). However, there is no direct evidence that MAA-absorbed energy can be transmitted to Chl *a* (D.P. Häder, personal communication). UV energy absorbed by MAAs is dissipated nonradiatively and is hardly available for photosynthesis (41).

Coeffect of UV and PAR in the photosynthesis of *G. lemaneiformis*

The positive effects of UV-A have been found in repairing UV-B-damaged DNA (42) as well as in enhancing growth rate (13) and enzyme activities (27,43). UV-B was also found to play positive roles in the recovery process of the photoinhibition in a brown alga *Dictyota dichotoma* (44). It is possible that the longer wavelength of the UV-B band may also play positive roles in influencing the photosynthesis. In *G. lemaneiformis*, the maximal photosynthetic rate driven by UV-A alone can reach up to 17–18% of that driven by PAR alone (Table 1, Fig. 6). However, when UV-A and PAR acted together under solar radiation, the contribution by UV-A to the photosynthesis was only found under limiting PAR levels by up to 8% (18) or to 10% (Fig. 6) of that triggered by the corresponding levels of PAR. High levels of solar UV-A damage PSII and down-regulate the photosynthesis driven by PAR. The 18% photosynthetic contribution only implies the capacity of UV-A-driven photosynthesis in contrast to the PAR-saturated photosynthetic rate. In addition, the stimulation and inhibition of photosynthesis by UVA can happen simultaneously, and the observed stimulation or inhibition of photosynthetic rate is dependent on the balance between these two processes. Under reduced levels of solar radiation when PAR limits photosynthesis, UV-A-related stimulation can be obvious due to less pronounced inhibition, and inhibition of PAR-driven photosynthesis by UV can make the positive effects of UV-A invisible at high levels of solar radiation (17). In other words, if $P_{UV\text{-}A}$ (photosynthesis driven by UV-A) > $P_{PAR\text{-}inhibition}$ (the UV-A-related inhibition of photosynthesis driven by PAR), UV-A shows a positive effect, and vice versa. When $P_{UV\text{-}A}$ and $P_{PAR\text{-}inhibition}$ become balanced, no significant effect of UV-A would be found. Therefore, negative, neutral and positive effects have been reported under different levels of solar radiation (5). Also, such balanced effects depend on nutrient availability. UV-A enhanced both inorganic carbon acquisition and growth rate under the phosphate (P)-replete condition, but reduced both under the P-limited condition in *G. lemaneiformis* (45). Consequently, neglect of UV during measurement of algal photosynthesis can either overestimate the rates under high levels of solar radiation or nutrient-limited conditions due to the neglected harms of UV, or underestimate the rate on cloudy days or nutrient-replete conditions due to ignored enhancement by UV-A.

Acknowledgements—This work was supported by the National Basic Research Program of China (No. 2009CB421207), National Natural Science Foundation of China (40930846 and 40876058 to K.G.) and the Ministry of Education (308015 to K.G.). We thank Prof. Donat Häder for helpful comments on the data during his visit to Xiamen University.

REFERENCES

1. Häder, D. P., H. D. Kumar, R. C. Smith and R. C. Worrest (2007) Effects of solar UV radiation on aquatic ecosystems and interactions with climate change. *Photochem. Photobiol. Sci.* **6**, 267–285.
2. Sinha, R. P., M. Klisch, A. Gröniger and D. P. Häder (2001) Responses of aquatic algae and cyanobacteria to solar UV-B. *Plant Ecol.* **154**, 219–236.
3. Weatherhead, E. C. and S. B. Andersen (2006) The search for signs of recovery of the ozone layer. *Nature* **441**, 39–45.
4. Han, T., Y. S. Han, J. M. Kain and D. P. Häder (2003) Thallus differentiation of photosynthesis, growth, reproduction, and UV-B sensitivity in the green alga *Ulva pertusa* (Chlorophyceae). *J. Phycol.* **39**, 712–721.
5. Helbling, E. W., K. Gao, R. J. Goncalves, H. Wu and V. E. Villafañe (2003) Utilization of solar ultraviolet radiation by phytoplankton assemblages from the Southern China Sea when exposed to fast mixing conditions. *Mar. Ecol. Prog. Ser.* **259**, 59–66.
6. Sass, L., C. Spetea, Z. Máté, F. Nagy and I. Vass (1997) Repair of UV-B-induced damage of photosystem II via de novo synthesis of the D1 and D2 reaction centre subunits in *Synechocystis* sp. PCC 6803. *Photosynth. Res.* **54**, 55–62.

7. Buma, A. G. J., P. Boelen and W. H. Jeffrey (2003) UVR-induced DNA damage in aquatic organisms. In *UV Effects in Aquatic Organisms and Ecosystems* (Edited by E. W. Helbling and H. E. Zagarese), pp. 291–327. The Royal Society of Chemistry, Cambridge.
8. Wu, H., K. Gao, V. E. Villafañe, T. Watanabe and E. W. Helbling (2005) Effects of solar UV radiation on morphology and photosynthesis of filamentous cyanobacterium *Arthrospira platensis*. *Appl. Environ. Microbiol.* **71**, 5004–5013.
9. Gao, K. and Z. Ma (2008) Photosynthesis and growth of *Arthrospira* (*Spirulina*) *platensis* (Cyanophyta) in response to solar UV radiation, with special reference to its minor variant. *Environ. Exp. Bot.* **63**, 123–129.
10. Fauchot, J., M. Gosselin, M. Levasseur, B. Mostajir, C. Belzile, S. Demers, S. Roy and P. Z. Villegas (2000) Influence of UV-B radiation on nitrogen utilization by a natural assemblage of phytoplankton. *J. Phycol.* **36**, 484–496.
11. Bischof, K., I. Gómez, M. Molis, D. Hanelt, U. Karsten, U. Lüder, M. Y. Roleda, K. Zacher and C. Wiencke (2006) Ultraviolet radiation shapes seaweed communities. *Rev. Environ. Sci. Biotechnol.* **5**, 141–166.
12. Huovinen, P. S., A. O. J. Oikari, M. R. Soimasuo and G. N. Cherr (2000) Impact of UV radiation on the early development of the giant kelp (*Macrocystis pyrifera*) gametophytes. *Photochem. Photobiol.* **72**, 308–313.
13. Henry, B. E. and K. L. Van Alstyne (2004) Effects of UV radiation on growth and phlorotannins in *Fucus gardneri* (Phaeophyceae) juveniles and embryos. *J. Phycol.* **40**, 527–533.
14. Wiencke, C., I. Gómez, H. Pakker, A. Flores-Moya, M. Altamirano, D. Hanelt, K. Bischof and F. Figueroa (2000) Impact of UV radiation on viability, photosynthetic characteristics and DNA of brown algal zoospores: Implications for depth zonation. *Mar. Ecol. Prog. Ser.* **197**, 217–229.
15. Han, T., J. A. Kong, Y. S. Han, S. H. Kang and D. P. Häder (2004) UV-A/blue light-induced reactivation of spore germination in UV-B irradiated *Ulva pertusa* (Chlorophyta). *J. Phycol.* **40**, 315–322.
16. Barbieri, E. S., V. E. Villafane and E. W. Helbling (2002) Experimental assessment of UV effects on temperate marine phytoplankton when exposed to variable radiation regimes. *Limnol. Oceanogr.* **47**, 1648–1655.
17. Gao, K., Y. Wu, G. Li, H. Wu, V. E. Villafañe and E. W. Helbling (2007) Solar UV radiation drives CO_2 fixation in marine phytoplankton: A double-edged sword. *Plant Physiol.* **144**, 54–59.
18. Gao, K. and J. Xu (2008) Effects of solar UV radiation on diurnal photosynthetic performance and growth of *Gracilaria lemaneiformis* (Rhodophyta). *Eur. J. Phycol.* **43**, 297–307.
19. Altamirano, M., A. Flores-Moya and F. L. Figueroa (2000) Long-term effects of natural sunlight under various ultraviolet radiation conditions on growth and photosynthesis of intertidal *Ulva rigida* (Chlorophyceae) cultivated in situ. *Bot. Mar.* **43**, 119–126.
20. Michler, T., J. Aguilera, D. Hanelt, K. Bischof and C. Wiencke (2002) Long-term effects of ultraviolet radiation on growth and photosynthetic performance of polar and cold-temperate macroalgae. *Mar. Biol.* **140**, 1117–1127.
21. Zou, D., J. Xia and Y. Yang (2004) Photosynthetic use of exogenous inorganic carbon in the agarophyte *Gracilaria lemaneiformis* (Rhodophyta). *Aquaculture* **237**, 421–431.
22. Neori, A., M. Vernet, O. Holm-hansen and F. T. Haxo (1986) Relationship between action spectra for Chlorophyll-*a* fluorescence and photosynthetic O_2 evolution in algae. *J. Plankton Res.* **8**, 537–548.
23. Neori, A., M. Vernet, O. Holm-Hansen and F. T. Haxo (1988) Comparison of chlorophyll far red and red fluorescence excitation-spectra with photosynthetic oxygen action spectra for photosystem II in algae. *Mar. Ecol. Prog. Ser.* **44**, 297–302.
24. Halldal, P. (1964) Ultraviolet action spectra of photosynthesis and photosynthetic inhibition in a green and a red alga. *Physiol. Plant.* **17**, 414–424.
25. Halldal, P. (1967) Ultraviolet action spectra in algology. *Photochem. Photobiol.* **6**, 445–460.
26. Beardall, J., P. Heraud, S. Roberts, K. Shelly and S. Stojkovic (2002) Effects of UV-B radiation on inorganic carbon acquisition by the marine microalga *Dunaliella tertiolecta* (Chlorophyceae). *Phycologia* **41**, 268–272.
27. Wu, H. and K. Gao (2009) Ultraviolet radiation stimulated activity of extracellular carbonic anhydrase in the marine diatom *Skeletonema costatum*. *Funct. Plant Biol.* **36**, 137–143.
28. Franklin, L. A. and R. M. Foster (1997) The changing irradiance environment: Consequences for marine macrophyte physiology, productivity and ecology. *Eur. J. Phycol.* **32**, 207–232.
29. Gao, K., P. Li, T. Watanabe and E. W. Helbling (2008) Combined effects of ultraviolet radiation and temperature on morphology, photosynthesis and DNA of *Arthrospira* (*Spirulina*) *platensis* (Cyanophyta). *J. Phycol.* **44**, 777–786.
30. Häder, D. P., M. Lebert, R. Marangoni and G. Colombetti (1999) ELDONET—European light dosimeter network hardware and software. *J. Photochem. Photobiol. B, Biol.* **52**, 51–58.
31. Jassby, A. D. and T. Platt (1976) Mathematical formulation of the relationship between photosynthesis and light for phytoplankton. *Limnol. Oceanogr.* **21**, 540–547.
32. Moroney, J. V., H. D. Husic and N. E. Tolbert (1985) Effect of carbonic anhydrase inhibitors on inorganic carbon accumulation by *Chlamydomonas reinhardtii*. *Plant Physiol.* **79**, 177–183.
33. Axelsson, L., C. Larsson and H. Ryberg (1999) Affinity, capacity and oxygen sensitivity of the two different mechanisms for bicarbonate utilization in *Ulva lactuca* L. (Chlorophyta). *Plant Cell Environ.* **22**, 969–978.
34. Beer, S. (1994) Mechanisms of inorganic carbon acquisition in marine macroalgae (with reference to the Chlorophyta). *Prog. Phycol. Res.* **10**, 179–207.
35. Axelsson, L., H. Ryberg and S. Beer (1995) Two modes of bicarbonate utilization in the marine green macroalga *Ulva lactuca*. *Plant Cell Environ.* **18**, 439–445.
36. Moisan, T. A. and B. G. Mitchell (2001) UV absorption by mycosporine-like amino acid in *Phaeocystis antarctica* Karsten induced by photosynthetically available radiation. *Mar. Biol.* **138**, 217–227.
37. Harris, D. G. and F. P. Zscheile (1943) Effects of solvent upon absorption spectra of chlorophylls *a* and *b*; their ultraviolet absorption spectra in ether solution. *Bot. Gaz.* **104**, 515–527.
38. Orellana, M. V., T. W. Petersen and G. Van Den Engh (2004) UV-excited blue auto- fluorescence of *Pseudo-nitzschia multiseries* (Bacillariophyceae). *J. Phycol.* **40**, 705–710.
39. Karsten, U., T. Sawall and C. Wiencke (1998) A survey of the distribution of UV-absorbing substances in tropical macroalgae. *Phycol. Res.* **46**, 271–279.
40. Sivalingam, P. M., T. Ikawa and K. Nisizawa (1976) Physiological roles of a substance 334 in algae. *Bot. Mar.* **19**, 9–21.
41. Shick, J. M. and W. Dunlap (2002) Mycosporine-like amino acids and related gadusols: Biosynthesis, accumulation, and UV-protective functions in aquatic organisms. *Annu. Rev. Physiol.* **64**, 223–262.
42. Pakker, H., C. A. C. Beekman and A. M. Breeman (2000) Efficient photoreactivation of UVBR-induced DNA damage in the sublittoral macroalga *Rhodymenia pseudopalmata* (Rhodophyta). *Eur. J. Phycol.* **35**, 109–114.
43. Viñegla, B., M. Segovia and F. L. Figueroa (2006) Effect of artificial UV radiation on carbon and nitrogen metabolism in the macroalgae *Fucus spiralis* L. and *Ulva olivascens* Dangeard. *Hydrobiologia* **560**, 31–42.
44. Flores-Moya, A., D. Hanelt, F. L. Figueroa, M. Altamirano, B. Viñegla and S. Salles (1999) Involvement of solar UV-B radiation in recovery of inhibited photosynthesis in the brown alga *Dictyota dichotoma* (Hudson) Lamouroux. *J. Photochem. Photobiol. B, Biol.* **49**, 129–135.
45. Xu, Z. and K. Gao (2009) Impacts of UV radiation on growth and photosynthetic carbon acquisition in *Gracilaria lemaneiformis* (Rhodophyta) under phosphorus-limited and replete conditions. *Funct. Plant Biol.* **36**, 1057–1064.